A Multi-view Opto-Xray Imaging System
Development and First Application in Trauma Surgery

Joerg Traub[1], Tim Hauke Heibel[1], Philipp Dressel[1], Sandro Michael Heining[2], Rainer Graumann[3], and Nassir Navab[1]

[1] Computer Aided Medical Procedures (CAMP), TUM, Munich, Germany
[2] Trauma Surgery Department, Klinikum Innenstadt, LMU Munich, Germany
[3] Siemens SP, Siemens Medical, Erlangen, Germany

Abstract. The success of minimally invasive trauma and orthopedic surgery procedures has resulted in an increase of the use of fluoroscopic imaging. A system aiming to reduce the amount of radiation has been introduced by Navab et al. [1]. It uses an optical imaging system rigidly attached to the gantry such that the optical and X-ray imaging geometry is identical. As an extension to their solution, we developed a multi-view system which offers 3D navigation during trauma surgery and orthopedic procedures. We use an additional video camera in an orthogonal arrangement to the first video camera and a minimum of two X-ray images. Furthermore, tools such as a surgical drill are extended by optical markers and tracked with the same optical cameras. Exploiting that the cross ratio is invariant in projective geometry, we can estimate the tip of the instrument in the X-ray image without external tracking systems. This paper thus introduces the first multi-view Opto- Xray system for computer aided surgery. First tests have proven the accuracy of the calibration and the instrument tracking. Phantom and cadaver experiments were conducted for pedicle screw placement in spinal surgery. Using a postoperative CT, we evaluate the quality of the placement of the pedicle screws in 3D.

1 Introduction

Mobile C-arm systems are established in everyday routines in orthopedic and trauma surgery. The trend toward minimally invasive applications increases the use of fluoroscopic images within surgery and thus the radiation dose [2,3]. Nowadays the combined use of mobile C-arms, that are capable of 3D reconstruction, and a tracking system provide navigation information during surgery, e.g. [4]. Systems using this technique use so called *registration free navigation* methods based on a mobile C-arm with 3D reconstruction capabilities tracked by an external optical tracking system. The imaging device is tracked and the volume is reconstructed in the same reference frame in which the instruments and the patient are tracked. Hayashibe et al. [5] combined the registration free navigation approach using an intra-operative tracked C-arm with reconstruction capabilities and in-situ visualization by volume rendered views from any arbitrary position of a swivel arm mounted monitor.

N. Ayache, S. Ourselin, A. Maeder (Eds.): MICCAI 2007, Part II, LNCS 4792, pp. 18–25, 2007.

Augmenting interventional imaging data using mirror constructions were proposed by Stetten et al. [6] for tomographic reflection on Ultrasound and Fichtinger et al. for navigated needle insertion based on CT [7] and MR [8].

Another approach for augmentation of intraoperative image data is the physical attachment of an optical camera to an X-ray source as proposed by Navab et al. [1]. It uses a single optical camera rigidly attached to the gantry such that the optical and X-ray imaging geometry is aligned. This enabled a real time video image and X-ray overlay that was registered by construction. No registration of the patient was required in their approach. This provided an accurate positioning and guidance of instruments in 2D. However, no depth control was possible. Thus their system was limited to applications where depth did not matter, like in intramedullary-nail locking as proposed by their group [9].

As an extension to their proposed system, we developed a system that is also capable of depth control during trauma surgery and orthopedic procedures using only one additional X-ray image and a second video camera that is rigidly attached to the C-arm. Furthermore, we implemented a system to track an instrument in 2D. Using cross ratio we estimate the position of the tip in the image. After one time calibration of the newly attached second video camera we are able to show the instrument tip in the orthogonal X-ray view. The feasibility of the system has been validated trough cadaver studies where we successfully identified all six pedicle screws placed using the procedure. The accuracy of the placement was validated using a postoperative CT.

2 System Setup

2.1 System Components

The system consists of an Iso3D C-arm (Siemens Medical, Erlangen, Germany) with two attached Flea video color cameras (Point Grey Research Inc., Vancouver, BC, Canada) (see figure 1). The first camera is attached as proposed earlier by Navab et al. using a double mirror construction with X-ray transparent mirrors [1]. The second camera is attached orthogonal to the gantry such that its view is aligned with the X-ray image after a 90 degrees orbital rotation of the C-arm (see figure 1). Furthermore, the system includes a standard PC with a framegrabber card to access the analog images of the C-arm. A custom developed visualization and navigation software is used (see section 2.3).

2.2 System Calibration

For both cameras the calibration process can be devided in two consecutive steps. In the first step the cameras are physically attached such that the optical center and axis virtually coincide with the X-ray imaging system at all time for the gantry mounted camera and at particular C-arm positions for the orthogonal mounted camera. The second step is to compute the homographies to align the video images with the X-ray images. For both video cameras the distortion is computed using the Matlab camera calibration toolbox and the images

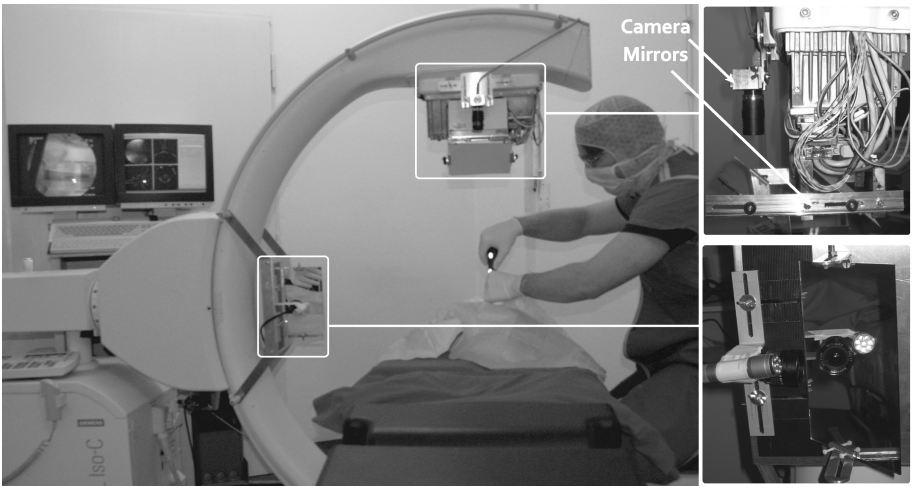

Fig. 1. The C-arm with two attached optical cameras. The first camera is attached to the gantry with a double mirror construction. The second camera is attached in an orthogonal direction with a single mirror construction.

are undistorted using Intel OpenCV library. The use of flat panel displays or standard distortion correction methods is recommended [1].

Notation. Since we have images at different positions of the C-arm superscript 0 denote cameras and images at a 0 degree orbital rotation and superscript 90 denote cameras and images acquired by the C-arm after an orbital rotation around 90 degree. Furthermore subscript x is used for X-ray, g for gantry mounted, and o for the orthogonal mounted cameras.

X-ray to Gantry Mounted Camera Calibration. Initially the gantry mounted camera is physically placed such, that its optical center and axis are aligned respectively with the X-ray source. This alignment is achieved by a bi-planar calibration phantom and mounting the camera using a double mirror construction. To superimpose the X-ray image onto the video image a homography $H_{I_g^0 \leftarrow I_x^0}$ is computed. Thanks to this homography the effects of X-ray distortions close to the image center are diminished. The procedure of the gantry mounted camera calibration is described in detail by Navab et al. [1].

X-ray to Orthogonal Mounted Camera Calibration. We constrained the attachment of the second camera to be orthogonal with respect to the gantry. This attachment provides best results for the depth navigation, assuming the instruments are always used down the beam as in the single camera navigation system [1]. The physical attachment and calibration of the second camera at alternative positions is also possible with the procedure described in this section.

[1] See `http://campar.in.tum.de/Events/VideoCamCSquare` for a video demonstration of the calibration and navigation procedure.

To acquire an X-ray image I_x^{90} corresponding to the view I_o^0 of the orthogonal mounted camera, we have to ensure that after an orbital rotation the optical center and axis of the X-ray gantry and the orthogonal camera are aligned. Since the gantry mounted camera is already physically aligned with the X-ray device, the problem can be reduced to physically aligning the gantry mounted and orthogonal mounted camera after rotation. This alignment is achieved with a bi-planar calibration pattern. A set of markers is placed on each plane such that subsets of two markers, one on each plane, are aligned in the image of the gantry mounted camera I_g^0 at the initial position of the C-arm (see figure 2(e)). In the next step, the C-arm is rotated by -90 degrees in orbital(see figure 2(c)). Now the orthogonal mounted camera is physically moved in six degrees of freedom, until all marker tuples from the calibration pattern are lined up in image I_o^{-90} in exactly the same way as they were for the gantry mounted camera (see figure 2(f)). Note that the calibration only has to be performed once the system is constructed. Once the system is built, the alignment is preserved by construction.

For a proper alignment of the X-ray image I_x^{90} at 90 degree rotation in orbital direction and the image I_o^0 of the orthogonal camera with no rotation, two homographies remain to be computed. A first homography $H_{I_g^{90} \leftarrow I_x^{90}}$ that maps the X-ray image I_x^{90} to the gantry mounted image I_g^{90} and a second homography $H_{I_o^0 \leftarrow I_g^{90}}$ mapping the image of the gantry mounted camera to the image of the orthogonal mounted camera. The final homography used to map the X-ray image I_x^{90} onto the orthogonal mounted camera image I_o^0 uses the hompgraphy $H_{I_o^0 \leftarrow I_x^{90}} = H_{I_o^0 \leftarrow I_g^{90}} \cdot H_{I_g^{90} \leftarrow I_x^{90}}$, a combination of the two homograpies computed earlier. Both homographies are computed using corresponding points in the images. Even though the gantry camera is rigidly mounted a second estimation of the homography $H_{I_g^{90} \leftarrow I_x^{90}}$ is determined to approximately compensate distortion effects of the X-ray image after rotation.

2.3 Navigation System

The navigation does not require any further calibration or registration procedure. The previously described calibration routine has to be performed only once while the system is built and it is valid as long as the cameras do not move with respect to the gantry.

For the navigation the acquisition of two X-ray images I_x^0 and I_x^{90} with a precise orbital rotation, such that the acquired images correspond to the images of the gantry attached camera I_g^0 and the orthogonal camera I_o^0, has to be ensured. Therefore an image I_o^0 of the second camera is captured before the rotation. Using image overlay techniques of this captured image I_o^0 and a live video image $I_g^{0 \rightarrow 90}$ during the orbital rotation with the homography $H_{I_o^0 \leftarrow I_g^{90}}$ applied, we ensure that the first camera has the same position and orientation as the second camera before the rotation. Thus the X-ray image I_x^{90} we take from this position corresponds to the captured image I_o^0. Furthermore, after precise rotation of the C-arm back to its original position, the orthogonal taken X-ray image I_x^{90} can be overlaid on the live image I_o^0 of the orthogonal mounted camera

by applying the computed homography $H_{I_o^0 \leftarrow I_x^{90}}$. The rotation back is ensured using combined X-ray and optical markers attached to the side of our surgical object that are visible in the X-ray image I_x^{90} and the image I_o^0 of the orthogonal camera. The acquisition of a second X-ray image I_x^0 at position zero and the use of the homography $H_{I_g^0 \leftarrow I_x^0}$ enables the lateral control using the gantry mounted camera (see figure 3(a). The image I_o^0 of the orthogonal camera is used by an instrument tracking module (see figure 2.4). The estimated distal end of the instrument in the orthogonal image I_g^0 is superimposed on the X-ray image I_x^{90} taken at 90 degree rotation (see figure 3(c)).

2.4 Instrument Tracking

The surgical tool is extended by three markers collinear arranged on the instrument axis. We use retro-reflective circular markers that are illuminated by an additional light source attached to the orthogonal camera. This setup results in the markers being seen by the orthogonal camera as bright ellipses, which can be easily detected by image thresholding. From the binary image all contours are extracted using the Intel OpenCV library. In a post-processing step we filter those contours having a low compactness value and those having a smaller area than a threshold (default values are 0.6 for the compactness and 50 pixels for the area). For all contours being retained by the filtering routine, the sub-pixel centroids are computed based on grayscale image moments. Finally those three contours yielding an optimal least squares line fitting are assumed to be the ones corresponding to our circular markers.

Having three collinear markers detected in the 2D image plane, we are able to compute the position of the instrument tip. Given the 3D geometry of our instrument, i.e. the position of the distal end of the instrument with respect to the other three markers, we compute the tip of the instrument in the image based on the cross-ratio.

$$cross = \frac{d_{12}d_{23}}{d_{13}d_{24}} = \frac{\Delta x_{12}\Delta x_{23}}{\Delta x_{13}\Delta x_{24}} = \frac{\Delta y_{12}\Delta y_{23}}{\Delta y_{13}\Delta y_{24}} \tag{1}$$

Here d_{ij} are the distances between the markers i and j, respectively between a marker and the tool tip. Investigating the distances in x- and y-direction separately gives us Δx_{ij} and Δy_{ij} where $\Delta x_{24} = |x_2 - x_4|$ and $\Delta y_{24} = |y_2 - y_4|$ contain the unknown coordinates x_4 and y_4 of the instrument tip. Since the X-ray image I_x^{90} is registered with the live video image I_o^0 of the second camera by $H_{I_o^0 \leftarrow I_g^{90}}$, we know exactly the position of the tip in the X-ray image I_x^{90} taken at 90 degree rotation (see figure 3(c)).

3 Experiments and Results

First the feasibility of the system was tested on a spine phantom. We used a tracked awl, a pedicle probe and a T-handle to place pedicle screws. Using an

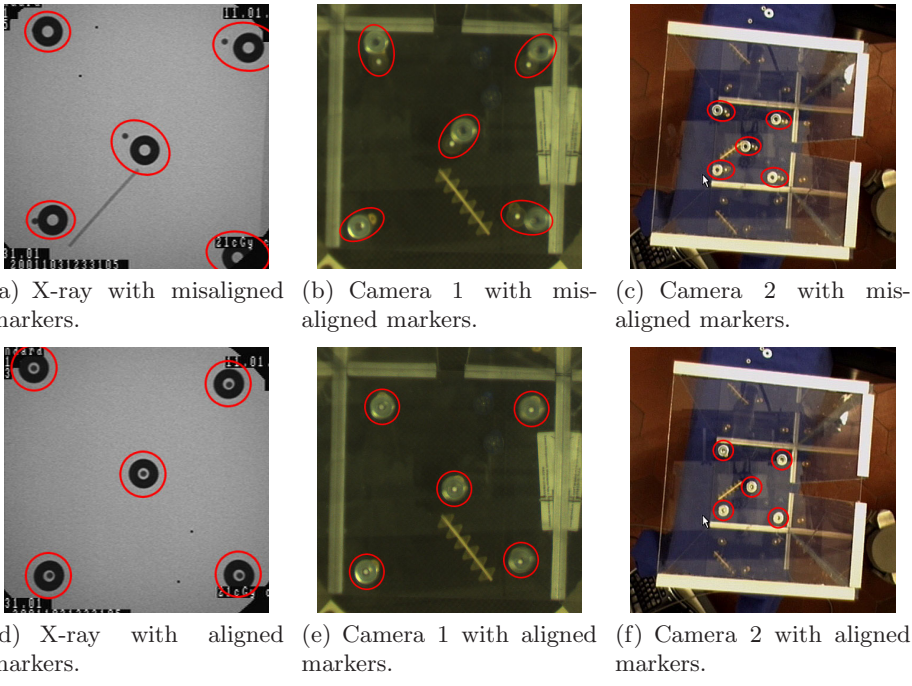

(a) X-ray with misaligned markers. (b) Camera 1 with misaligned markers. (c) Camera 2 with misaligned markers.

(d) X-ray with aligned markers. (e) Camera 1 with aligned markers. (f) Camera 2 with aligned markers.

Fig. 2. The calibration phantom in the different imaging systems

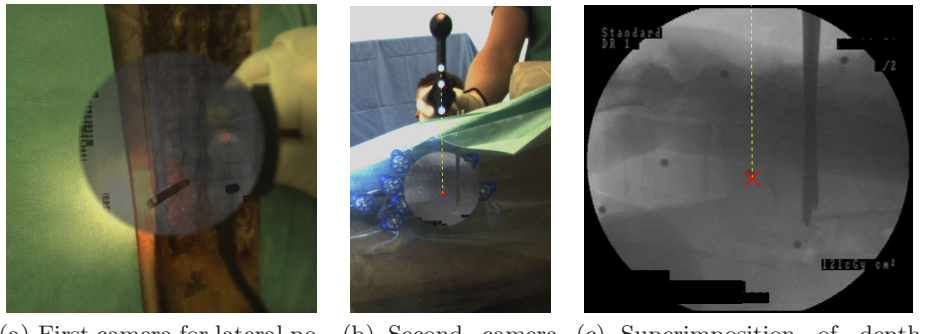

(a) First camera for lateral positioning. (b) Second camera for depth tracking. (c) Superimposition of depth tracking onto the X-ray image.

Fig. 3. The navigation interface including the lateral positioning of the instrument and the depth control using cross ratio

orthogonal control X-ray image we could visually verify the accuracy of the depth navigation.

In a cadaver experiment we placed eight pedicle screws (Universal Spine System USS, Synthes, Umkirch) with a diameter of 6.2 mm in four vertebrae of the thoracic and lumbar spine (Th12-L3). The surgical procedure was carried out

in three steps using a pedicle awl to open the cortical bone, a pedicle probe to penetrate the pedicle, and a T-handle for screw implantation. For the guided procedure both augmented views, the one for 2D positioning (see figure 4(a)) and the one for depth control (see figure 4(b)), were used simultaneously. After aligning the optical axis of the C-arm imaging system with the desired direction of the pedicle screws, the acquisition of only two X-ray images was required for each pedicle screw. This is a considerable reduction of radiation compared to standard fluoro based procedure.

The accuracy of the pedicle screw placement was verified by a postinterventional CT-scan ((see figure 4(c) and 4(d))) using a clinical scale proposed by Arand et al. [10]. Five pedicle screws were classified by an medical expert to be in group A, i.e. central screw position without perforation. The other three screws were classified to be in group B, i.e. lateral screw perforation within thread diameter. For none of the eight pedicle screws a medial perforation in direction of the spinal canal occurred.

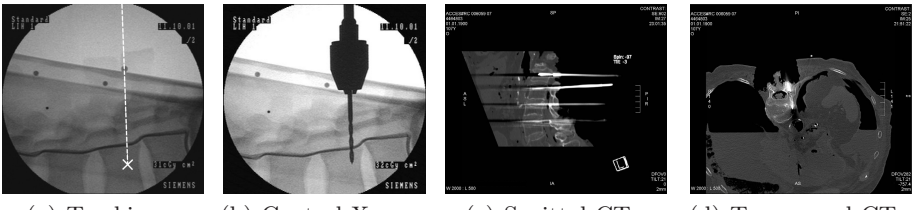

(a) Tracking. (b) Control X-ray. (c) Sagittal CT. (d) Transversal CT.

Fig. 4. Evaluation of the developed system using a control X-ray I_x^{90} and postinterventional CT data

4 Discussion

We have extended a real-time video augmented X-ray to a multi-view Opto-Xray imaging system. The previously proposed single camera augmentation system has proven to be efficient for trauma surgery and orthopedic applications where 3D did not matter, e.g. intramedullary-nail locking. The original system was extended by a second camera mounted in an orthogonal arrangement to the first camera. The second camera, thanks to a calibration and navigation protocol, enables applications for trauma surgery that are only possible at the moment using permanent fluoroscopic imaging or C-arm with 3D reconstruction capabilities and external tracking systems, both resulting in considerable increase of the radiation dose. Our newly developed system proved that it is possible to perform these procedures with the use of only two X-ray images and the assumption that the object does not move after the X-ray acquisition. If the object moves, simply another pair of X-rays has to be acquired. Using our proposed system and calibration procedure we are neither limited to exactly two cameras nor to a specific physical arrangement. First cadaver experiments demonstrated that the new system can be easily integrated into the clinical workflow while reducing the

radiation dose compared to other methods. The observed accuracy during the experiments is clinically acceptable. Further work will compare quantified results with CT based and C-arm based standard navigation techniques. The invention and implementation of a system for real-time augmentation of orthogonal X-ray views of a surgery, opens the way for development of new C-arms with integrated 3D navigation capabilities with no further need for online calibration.

Acknowlegments. Special thanks to Siemens Medical SP and Benjamin Ockert.

References

1. Navab, N., Mitschke, M., Bani-Hashemi, A.: Merging visible and invisible: Two camera-augmented mobile C-arm (CAMC) applications. In: IWAR, pp. 134–141 (1999)
2. Boszczyk, B.M, Bierschneider, M., Panzer, S., Panzer, W., Harstall, R., Schmid, K., Jaksche, H.: Fluoroscopic radiation exposure of the kyphoplasty patient. European Spine Journal 15, 347–355 (2006)
3. Synowitz, M., Kiwit, J.: Surgeon's radiation exposure during percutaneous vertebroplasty. J. Neurosurg. Spine. 4, 106–109 (2006)
4. Siewerdsen, J.H., Moseley, D.J., Burch, S., Bisland, S.K., Bogaards, A., Wilson, B.C., Jaffray, D.A.: Volume ct with a flat-panel detector on a mobile, isocentric c-arm: Pre-clinical investigation in guidance of minimally invasive surgery. Medical Physics 32(1), 241–254 (2005)
5. Hayashibe, M., Suzuki, N., Hattori, A., Otake, Y., Suzuki, S., Nakata, N.: Surgical navigation display system using volume rendering of intraoperatively scanned ct images. Computer Aided Surgery 11(5), 240–246 (2006)
6. Stetten, G.D., Chib, V.: Magnified real-time tomographic reflection. In: Niessen, W.J., Viergever, M.A. (eds.) MICCAI 2001. LNCS, vol. 2208, Springer, Heidelberg (2001)
7. Fichtinger, G., Deguet, A., Masamune, K., Balogh, E., Fischer, G.S., Mathieu, H., Taylor, R.H., Zinreich, S.J., Fayad, L.M.: Image overlay guidance for needle insertion in ct scanner. IEEE Transactions on Biomedical Engineering 52(8), 1415–1424 (2005)
8. Fischer, G.S., Deguet, A., Schlattman, D., Taylor, R., Fayad, L., Zinreich, S.J., Fichtinger, G.: Mri image overlay: Applications to arthrography needle insertion. In: Medicine Meets Virtual Reality (MMVR), vol. 14 (2006)
9. Heining, S.M., Wiesner, S., Euler, E., Mutschler, W., Navab, N.: Locking of intramedullary nails under video-augmented flouroscopic control: first clinical application in a cadaver study. In: Proceedings of CAOS, Montreal, Canada (2006)
10. Arand, M., Schempf, M., Fleiter, T., Kinzl, L., Gebhard, F.: Qualitative and quantitative accuracy of caos in a standardized in vitro spine model. Clin. Orthop. Relat. Res. 450, 118–128 (2006)